HOKKAIDO UNIVERSITY

Title	Ruxolitinib protects skin stem cells and maintains skin homeostasis in murine graft-versus-host disease
Author(s)	Takahashi, Shuichiro; Hashimoto, Daigo; Hayase, Eiko et al.
Citation	Blood, 131(18), 2074-2085 https://doi.org/10.1182/blood-2017-06-792614
Issue Date	2018-05-03
Doc URL	https://hdl.handle.net/2115/73806
Type	journal article
File Information	blood-2017-06-792614-1.pdf

Hokkaido University Collection of Scholarly and Academic Papers : HUSCAP

Supplementary Methods

Mice. Female C57BL/6 (B6, H-2^b), BALB/c (H-2^d) and B6D2F1 (BDF1, H-$2^{b/d}$) were purchased from Japan CLEA (Tokyo, Japan). B6-*Lgr5-EGFP-IRES-creER*^{T2} (B6-*Lgr5*$^{EGFP\text{-}cre/ER}$, H-2^b), B6.*Cg-Tg (Lck-cre) 548Jxm* (B6-*Lck-cre,* H-2^b), B6.*Cg-Gt(ROSA)26Sor*$^{tm14(CAG\text{-}tdTomato)Hze/J}$ (B6-R26^{tdTomato}, H-2^b) were purchased from Jackson Laboratory (Bar Harbor, ME). Interleukin-17A (IL-17A) fate mapping mice with the B6 background (Il17a^{Cre}×R26^{eYFP}, H-2^b) were generated, as previously reported (reference #19 in main text). In all experiments, animals were allocated randomly for each experimental group, ensuring the mean body weight in each group was similar. All animal experiments were performed under the auspices of the Institutional Animal Care and Research Advisory Committee (approval number; 12-0106).

Cell isolation from the skin. Depilated entire back skin was harvested and its subcutaneous fat layers were scraped off until translucent skin was exposed. Samples were cut into 2-4 mm pieces with scissors and incubated for 1 h at 37ºC in Dulbecco's modified Eagle medium (DMEM) and 1 μg/mL collagenase type 4 (Sigma-Aldrich). After the incubation, samples were homogenized and passed through a 70-μm cell strainer.

Flow cytometry. Monoclonal antibodies (mAbs) used for flow cytometry are provided in Table S1. 4',6-Diamidino-2-phenylindole (DAPI, Dojindo Laboratories, Kumamoto, Japan) and Live/Dead Fixable Viability Dye eFluor 450 (eBioscience, San Diego, CA) were used to exclude dead cells. CountBright

absolute counting beads (Invitrogen, Carlsbad, CA) were used for cell count. For analysis of apoptosis, cells were stained with FITC-conjugated Annexin V (BioLegend, San Diego, CA) in Annexin binding buffer (BioLegend). Ki-67 and Foxp3 was stained after permeabilization using Foxp3 staining buffer (Thermo Fisher Scientific, Waltham, MA) to evaluate donor T cell proliferation and expansion of donor regulatory T cells, respectively. To evaluate cytokine production, cells were stimulated by 50 ng/mL of phorbol 12-myristate 13-acetate (Sigma-Aldrich) and 1 μg/mL of ionomycin (Sigma-Aldrich) for 6 h at 37ºC, and Golgi-stop (BD Pharmingen) was added for the last 5 h. After staining surface markers, cells were fixed and permeabilized using a Cytofix/Cytoperm kit (BD Biosciences, San Jose, CA), followed by interferon-γ (IFN-γ) staining. Serum levels of IFN-γ were measured using a BD Cytometric Bead Array kit (BD Biosciences). Labeled cells were analyzed using a FACS CantoII (BD Biosciences) and FlowJo software (TreeStar, Ashland, OR).

Histology. Tissue samples were fixed with 4% paraformaldehyde overnight, embedded in paraffin, and stained with hematoxylin and eosin (H&E). Images were acquired at room temperature using a BX50 microscopy (Olympus, Tokyo, Japan) with a 10×/0.30 NA, 20×/0.45 NA, or 40×/0.95 NA objective lens. We also made the section of rolled skin samples to count the number of hair follicles. The number of hair follicles standardized with sample length (cm) was compared among mice.

Immunofluorescent study. Entire back skin was rolled and incubated with 4% paraformaldehyde overnight. For antigens retrieval, sections of rolled skin were heated in Target Retrieval Solution pH 9 (Dako Japan, Kyoto, Japan) at 105 °C for 20 min. The sections were then treated with blocking reagents containing 10% goat serum for 30 min, followed by incubation with primary antibodies listed in Table S1 at 4 °C overnight. The primary Abs were visualized by incubating with Alexa Fluor 488 or 555 conjugated goat anti-chicken polyclonal Abs or goat anti-rabbit polyclonal Abs for 1 h and nuclei were stained with DAPI. Images were acquired with a Fluoview FV1000 confocal microscopy (Olympus). Images were processed with Adobe Photoshop CC 2017.

Supplementary Legends

Figure S1. Emergence of keratinocytes derived from Lgr5^{+} HFSCs in wound repair

(**A, B**) Full-thickness wounds were made on the back skin of naïve B6-*Lgr5*$^{EGFP\text{-}cre/ER}$ × R26^{tdTomato} mice after Cre recombination and skin samples were obtained 10 days after wounding. (**A**) H&E staining of the skin harvested from the margin of the wound and regenerated epithelium. The regenerated epithelium was marked with a double-headed arrow. Magnification, 10×. Scale bar, 100 μm. (**B**) Immunofluorescent staining of the area in the black rectangle in (**A**) and intact skin with anti-RFP (red) mAbs and DAPI (blue). Dotted lines show epidermal-dermal junction. Magnification, 20×. Scale bar, 100 μm.

Figure S2. Topical administration of ruxolitinib suppresses IFNγ-induced expression of *Cxcl9* in the skin

IFN-γ (0.1 μg) or PBS was injected into the pinna of naive B6 mice on days +1 and +3. Control vaseline (Ctrl) or ruxolitinib ointment (Ruxo) was administered on the ears from day +1 to day +4. Expression levels of *Cxcl9* in ear samples harvested on day +5 were measured by Q-PCR (n=4-6 /group). One-way ANOVA followed by Tukey's post-test was used to compare the data. **P<0.01, ***P<0.005. Data represent the mean ± SEM from 2 independent experiments.

Figure S3. Topical ruxolitinib promotes wound healing made on day +28 after allogeneic SCT

B6 mice were transplanted as in Figure 1. Wounding was performed on day +28. Wound areas were measured daily for 7 days after wounding (n=6-8 /group). Data from 2 independent experiments are combined and shown as the mean ± SEM. **P<0.01.

Figure S4. Topical ruxolitinib does not mitigate the steroid toxicities on HFSCs and fat layer of the skin

Lethally irradiated B6-*Lgr5*$^{EGFP\text{-}cre/ER}$ mice were transplanted with 20 × 10^6 G-CSF mobilized splenocytes from syngeneic B6 mice on day 0. Betamethasone valerate ointment 0.12% (BMV) with or without ruxolitinib ointment was administered onto shaved back skin from day +1. The numbers of Lgr5$^+$ HFSCs (**A**, n=5 /group) and representative images of H&E staining of treated skin (**B**, Scale bar: 100 μm) on day +14 after syngeneic SCT. ns: not significant.

Figure S5. Systemic administration of ruxolitinib, not corticosteroid protects HFSCs against GVHD

Lethally irradiated B6-*Lgr5*$^{EGFP\text{-}cre/ER}$ were transplanted with 20 × 10^6 G-CSF mobilized splenocytes from allogeneic (Allo) BALB/c mice on day 0. Ctrl or ruxolitinib ointment was administered onto shaved back skin from day +1. For systemic therapy, 10 mg/kg prednisolone (PSL, once daily) or 30 mg/kg ruxolitinib (Ruxo, twice daily) were orally administered from day +1 after SCT. A group of recipients were treated with ruxolitinib ointment in combination with systemic ruxolitinib. Numbers of Lgr5$^+$ HFSCs (**A**) and donor T

cells in the PSL-treated skin (**B**) on day +14 from two independent experiments were combined and shown as the mean ± SEM (n=5-6 /group). *P<0.05, **P<0.01, ns: not significant.

Figure S6. Systemic administration of ruxolitinib ameliorates systemic GVHD

B6 mice were transplanted as in Figure 1. (**A-C**) Ruxolitinib or vehicle was orally administered from day +1 after SCT. Serum levels of TNFα on day +7 (**A**), numbers of donor regulatory T cells in the spleen on day +14 (**B**), and clinical GVHD scores on day +7 (**C,** n=5-6 /group). Treg: regulatory T cells, *P<0.05, **P<0.01, ***P<0.005.

Figure S7. The effect of topical ruxolitinib is limited in the treated skin

(**A-D**) Mice were treated with Ctrl or Ruxo from day +1 after SCT. **(A)** Numbers of donor T cells in the spleen on day +14 after SCT (n=6-7 /group). **(B)** Numbers of $CD4^+CD8^+$ double positive cells in the thymus on day + 28 after SCT. (**C**) Clinical GVHD scores after SCT (n=5 /group). (**D**) Pathology scores of the non-treated skin (n=5 /group), liver, small intestine, and colon (n=7-8 /group) on day + 28 after SCT. Mann-Whitney U testes or One-way ANOVA followed by Tukey's post-test was used to compare the data. Data represent the mean ± SEM from 2-3 independent experiments. *P<0.05, **P<0.01, ***P<0.005, ns: not significant.

Figure S8. Oral administration of ruxolitinib protects $CK15^+$ epidermal stem cells in RLPs after

allogeneic SCT.

Lethally irradiated B6 mice were transplanted as in Fig. S3. Vehicle (Ctrl) or ruxolitinib (Ruxo) at a dose of 60 mg/kg/day was orally given twice daily from day +1 after SCT. Immunofluorescent staining of CK15 (red) and DAPI (blue) in lingual sections harvested on day +9 after SCT. Magnification, 40×. Scale bar, 25 μm.

Figure S9. Therapeutic administration of systemic ruxolitinib ameliorates established systemic acute GVHD.

Lethally irradiated B6 mice were transplanted as in Figure 1. Ruxolitinib or vehicle were orally administered twice daily from day +9 after SCT. Survival rate (**A**) and clinical GVHD scores (**B**, the mean ± SEM) from two independent experiments were combined (n=8-10 /group). *P<0.05, **P<0.01.

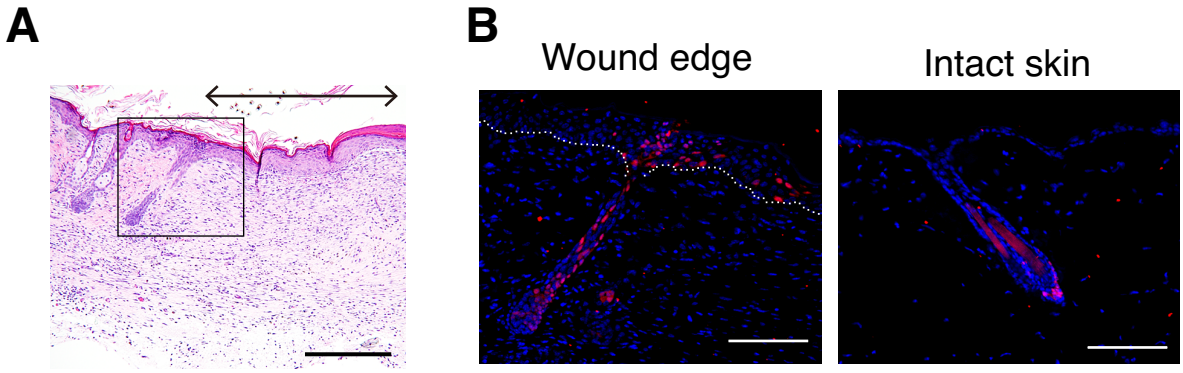


Figure S1.

Takahashi, et al.

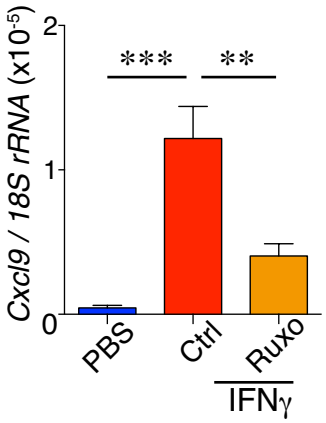


Figure S2.

Takahashi, et al.

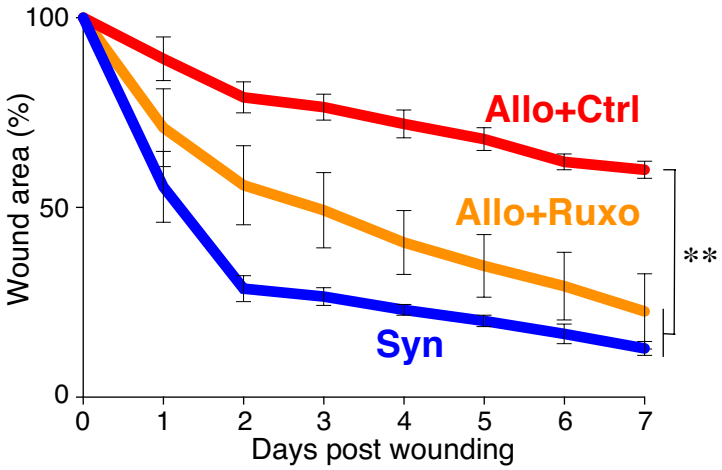


Figure S3.

Takahashi, et al.

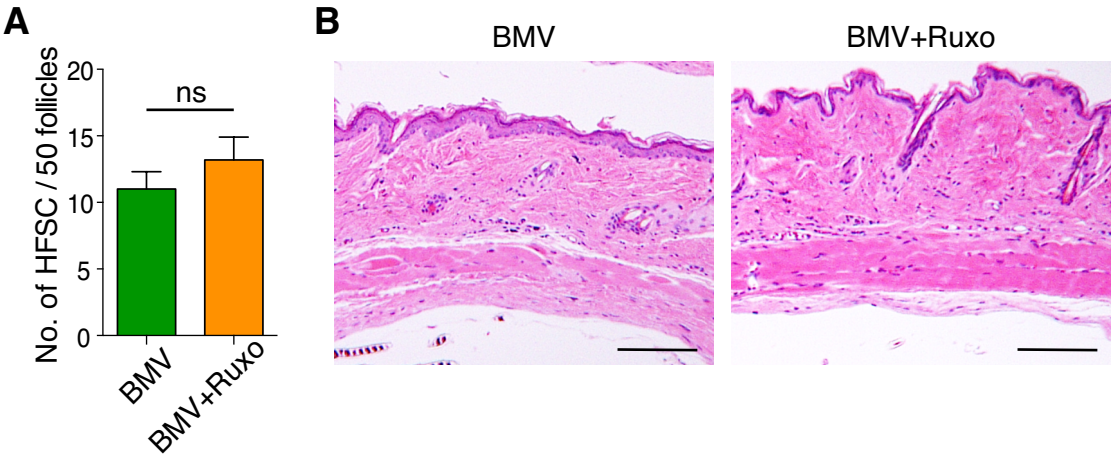


Figure S4.

Takahashi, et al.

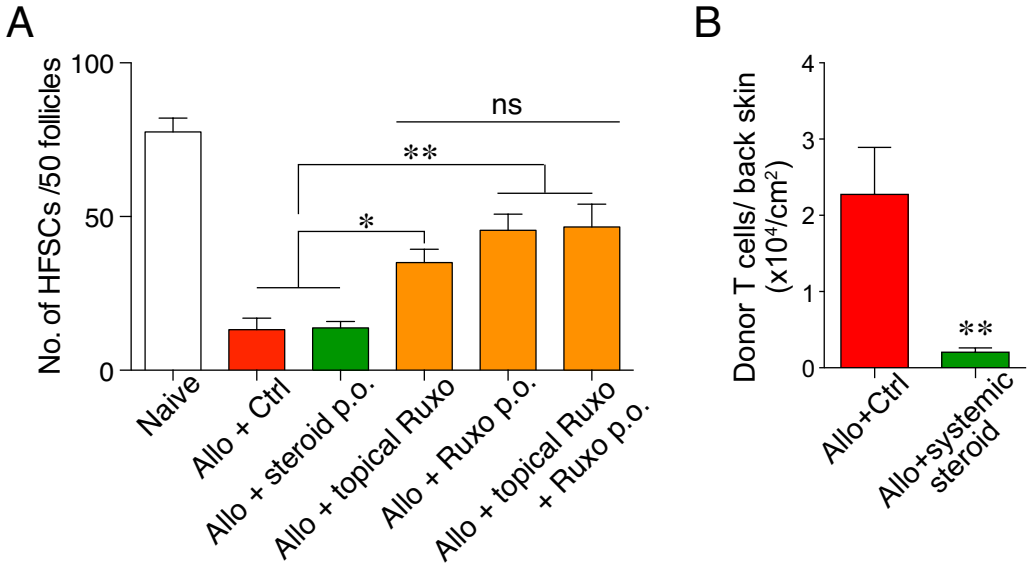


Figure S5.

Takahashi, et al.

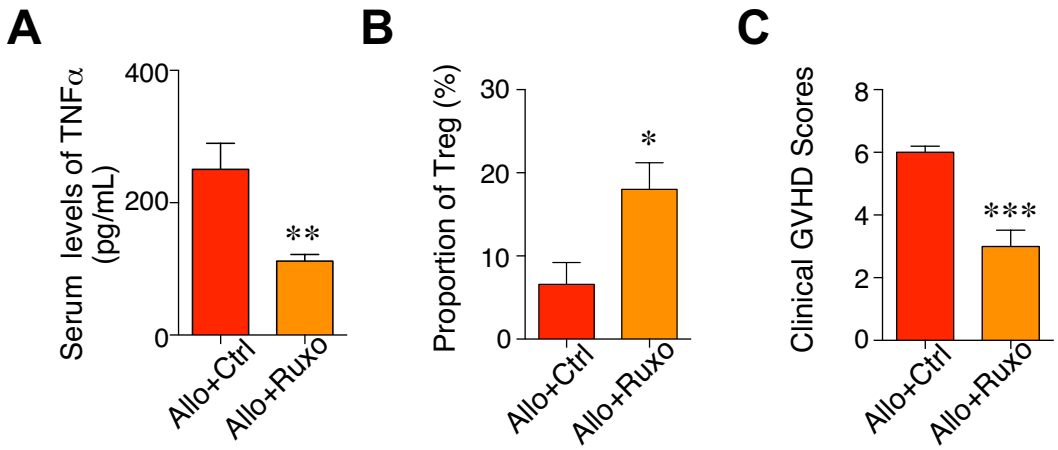


Figure S6.

Takahashi, et al.

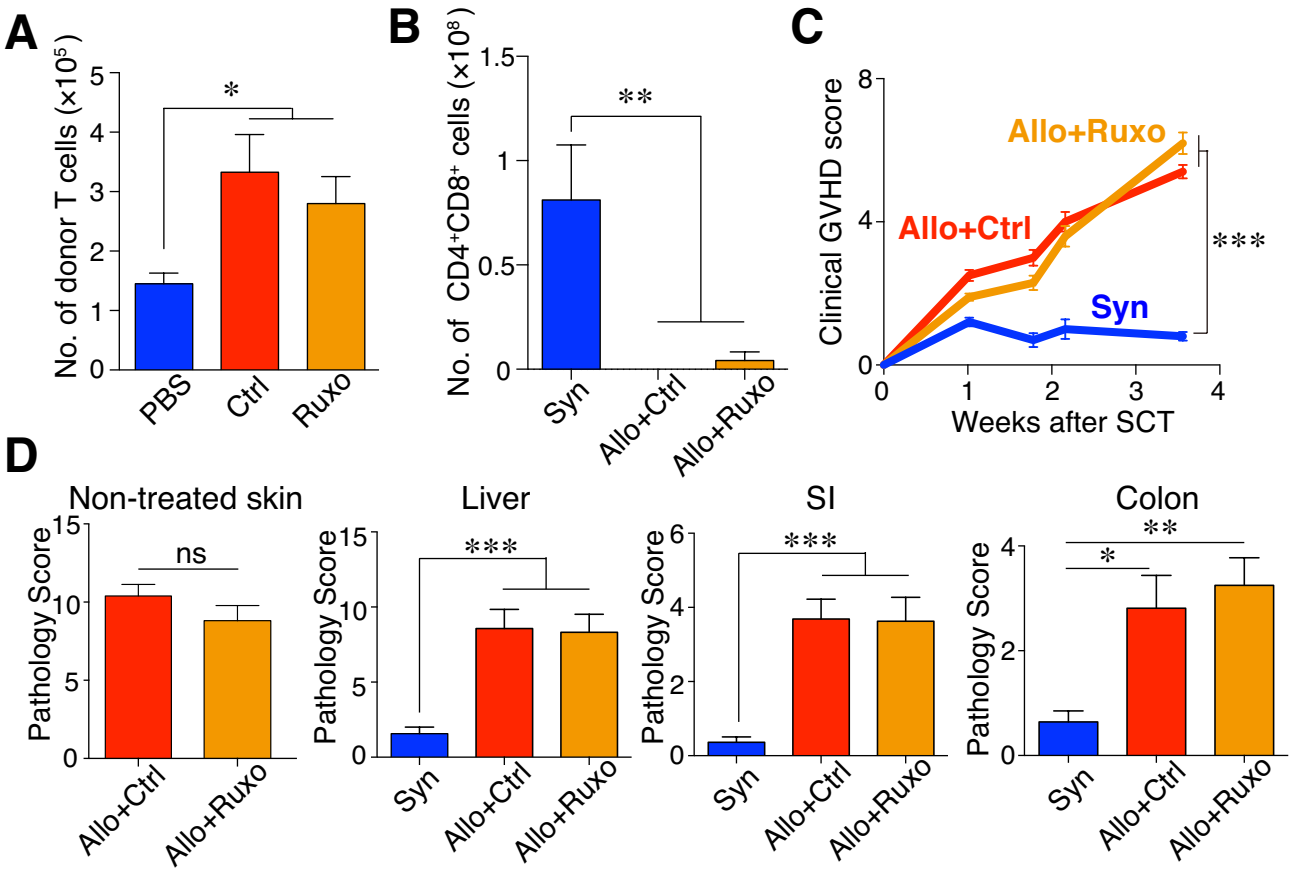


Figure S7.

Takahashi, et al.

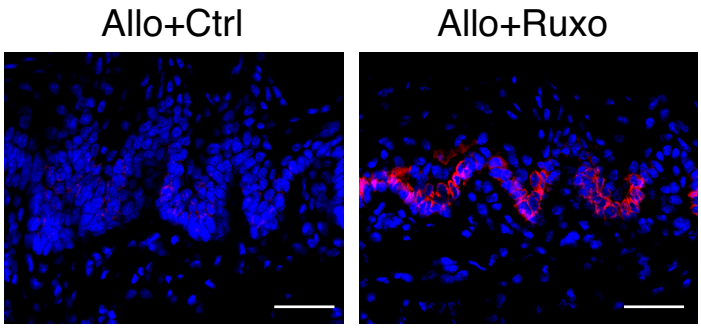


Figure S8.

Takahashi, et al.

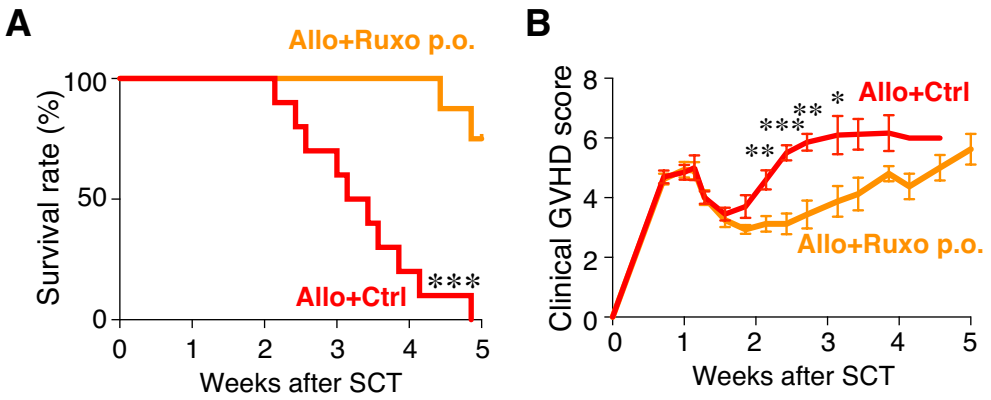


Figure S9.

Takahashi, et al.

Table S1. List of primary antibodies used in flow cytometry and immunofluorescent studies

Flow cytometry

Target Ag	Clone	Fluorochrome	Supplier	Catalog#	
TCRβ	H57-597	FITC	BD	553171	Nature. 2000; 406(6795):524-527.
H-2Kd	SF1-1.1	FITC	BD	553565	J Immunol. 1996;157(6):2455-2461.
CXCR3	CXCR3-173	PE	BD	550633	J Clin Invest. 1998; 101(4):746-754.
Ki-67	16A8	PE	BioLegend	652403	J Immunol. 2015; 194(11): 5529-38.
Foxp3	FJK-16s	PE	eBioscience	12-5773-82	J Immunol. 2008; 181(4): 2382-91.
CD11b	M1/70	PerCP-Cy5.5	BD	561114	Immunity. 2013 Apr 18;38(4):792-804.
CD4	GK1.5	PE-Cy7	BioLegend	100422	J Immunol. 2014; 192(1):178-88.
IFN-γ	XMG1.2	APC	BioLegend	505810	Nat Med. 2010; 6(6):701-7.
TCRβ	H57-597	APC	BD	554413	Science. 1994; 266(5188):1208-1212.
CD45	30-F11	APC-Cy7	BD	557659	Nat Med. 2000; 6(11):1212-1213
CD8a	53-6.7	BV510	BioLegend	100752	J Immunol. 2010; 185(2):998-1004.

Immunofluorescent studies

Target Ag	Clone	Supplier	Catalog#	
GFP	polyclonal	abcam	ab13970	J Clin Invest. 2016; 126:3104-3116.
Cytokeratin 15	ERP1614Y	abcam	ab52816	J Cell Sci. 2013; 126:5111-5.
RFP	polyclonal	abcam	ab34771	Nat Immunol. 2015; 16:153-60.
SOX9	polyclonal	Thermo Fisher Scientific	PA5-23383	
Ki-67	SP6	Thermo Fisher Scientific	MA5-14520	J Immunol. 2016; 196(4):1700-10.

Table S2. List of primer and probe sequences used in Q-PCR

Gene		Sequence
18S rRNA	Forward	5'- GCTCTTTCTCGATTCCGTGGG-3'
	Reverse	5'-ATGCCAGAGTCTCGTTCGTTATC-3'
	Probe	5'-CTCCACCAACTAAGAACGGCCATGCACC-3'
Cxcl9	Forward	5'-TCGAGGAACCCTAGTGATAAGGA-3'
	Reverse	5'-CGTTCTTCAGTGTAGCAATGATTTCA-3'
	Probe	5'-AGCACCAGCCGAGGCACGATCCA-3'
Cxcl10	Forward	5'-TGACGGGCCAGTGAGAATGA-3'
	Reverse	5'-CATCGTGGCAATGATCTCAACAC-3'
	Probe	5'-ATCATCCCTGCGAGCCTATCCTGCCC-3'
Cxcl11	Forward	5'-TGCTCAAGGCTTCCTTATGTTCA-3'
	Reverse	5'-GCCTTCATAGTAACAATCACTTCAAC-3'
	Probe	5'-CGCTGTCTTTGCATCGGCCCCGG-3'